



NMDAR antagonists suppress tumor progression by regulating tumor-associated macrophages

Dongchen Yuan^{a,1}, Jing Hu^{b,c,1,2} , Xiaoman Ju^{a,1}, Eva Maria Putz^d , Simin Zheng^a, Stephane Koda^a, Guowei Sun^a, Xiaoran Deng^e, Zhipeng Xu^f , Wei Nie^g, Yang Zhao^{h,i} , Xianyang Li^j, William C. Dougall^k, Simin Shao^a , Yan Chen^a, Renxian Tang^a , Kuiyang Zheng^{a,2} , and Juming Yan^{a,2}

Edited by Douglas Hanahan, Swiss Federal Institute of Technology Lausanne, Lausanne, Switzerland; received February 8, 2023; accepted October 4, 2023

Neurotransmitter receptors are increasingly recognized to play important roles in anti-tumor immunity. The expression of the ion channel N-methyl-D-aspartate receptor (NMDAR) on macrophages was reported, but the role of NMDAR on macrophages in the tumor microenvironment (TME) remains unknown. Here, we show that the activation of NMDAR triggered calcium influx and reactive oxygen species production, which fueled immunosuppressive activities in tumor-associated macrophages (TAMs) in the hepatocellular sarcoma and fibrosarcoma tumor settings. NMDAR antagonists, MK-801, memantine, and magnesium, effectively suppressed these processes in TAMs. Single-cell RNA sequencing analysis revealed that blocking NMDAR functionally and metabolically altered TAM phenotypes, such that they could better promote T cell- and Natural killer (NK) cell-mediated anti-tumor immunity. Treatment with NMDAR antagonists in combination with anti-PD-1 antibody led to the elimination of the majority of established preclinical liver tumors. Thus, our study uncovered an unknown role for NMDAR in regulating macrophages in the TME of hepatocellular sarcoma and provided a rationale for targeting NMDAR for tumor immunotherapy.

tumor | NMDA receptor | macrophages | tumor microenvironment | ROS

The immunosuppressive tumor microenvironment (TME) leads to tumor immune evasion and acquired resistance to cancer immunotherapy (1, 2). Checkpoint inhibitor therapies, particularly PD-1/PD-L1 inhibitors, elicit durable responses across a broad range of cancers. However, only a subset of patients within each of these cancers respond to treatment (3). Therefore, overcoming immunosuppressive mechanisms is crucial for developing more effective immunotherapies and treatment combination strategies.

Tumor-associated macrophages (TAMs) represent the most abundant immune population in the TME. While macrophages displaying M1-like features can produce pro-inflammatory cytokines and stimulate effector lymphocyte activities, TAMs often display M2-like features characterized by the production of immunosuppressive molecules. Clinically, high infiltration of TAMs is associated with unfavorable prognosis in most tumors (4). TAM-mediated immunosuppression occurs via many different pathways, including the production of immunosuppressive cytokines, immune checkpoint molecules, and metabolic regulation (4–7). Concerning metabolism, M2-like macrophages exhibit a high demand for glutamine, and employ fatty acid oxidation and oxidative phosphorylation (OXPHOS), while M1-like macrophages favor glycolysis and fatty acid synthesis (8). Given the phenotypic plasticity of TAMs, modulating their metabolism represents a potential approach to redirect TAMs toward tumoricidal phenotypes.

N-methyl-D-aspartate receptor (NMDAR) is a heterotetrameric protein comprising two obligatory NR1 subunits and two regulatory subunits (NR2A/B/C/D, NR3A/B) (9). NMDAR functions as a calcium, potassium, and sodium channel, and the NR1 subunit is required for the calcium conductivity of the channel. Glutamate and N-methyl-D-aspartate (NMDA) are natural agonists of NMDAR. The binding of ligands to NMDAR leads to the opening of the channel allowing the influx of calcium and sodium, and the efflux of potassium. The ion channel pore of NMDAR can be blocked by antagonists such as dizocilpine (MK-801) and memantine (MEM) (10–12). MK-801 has a higher affinity and longer dwell time on NMDAR, while MEM binds weakly to the ion channel (13). In addition, the ion permeability of NMDAR is regulated by ions such as Zn²⁺ and Mg²⁺. Several lines of evidence suggest that NMDAR is expressed by mouse and human macrophages and that its inhibition alters macrophage phenotypes (14, 15). However, it remains largely unknown whether targeting NMDAR could enhance the efficacy of cancer immunotherapy by modulating TAM. In this study, we find that activation of NMDAR in macrophages in the TME altered their functions and metabolism and enhanced expression of immune suppressive factors, leading to tumor immune evasion.

Significance

Glutamate is well known for its roles in intracellular metabolism processes, in addition to being one of the most indispensable neurotransmitters. Here, we identified a role for the glutamate receptor NMDAR (N-methyl-D-aspartate receptor) in regulating macrophage in the TME (tumor microenvironment). We found that blocking NMDAR with the antagonists suppressed tumor progression by altering the immune cell, especially the macrophage phenotype, function, and metabolism in the TME of hepatocellular sarcoma. Furthermore, the combination of NMDAR antagonists and anti-PD-1 antibody led to the rejection of established hepatocellular sarcoma. Subsequently, clinically approved drugs of NMDAR antagonists (memantine, ifenprodil tartrate) suppress tumor progression, indicating the clinical importance for immunotherapy.

Author contributions: D.Y., J.H., K.Z., and J.Y. designed research; X.J., S.Z., G.S., S.S., Y.C., and J.Y. performed research; Z.X., W.N., Y.Z., and X.L. contributed new reagents/analytic tools; X.D. and J.Y. analyzed data; and E.M.P., S.K., W.C.D., R.T., K.Z., and J.Y. wrote the paper.

Competing interest statement: X.L. is an employee of OriCell Therapeutics. W.C.D. is a member of the EpimAb Biotherapeutics scientific advisory board and holds patents related to the Receptor Activator of Nuclear Factor- κ B Ligand (RANKL) pathway. No potential conflicts of interest were disclosed by the other authors.

This article is a PNAS Direct Submission.

Copyright © 2023 the Author(s). Published by PNAS. This article is distributed under [Creative Commons Attribution-NonCommercial-NoDerivatives License 4.0 \(CC BY-NC-ND\)](https://creativecommons.org/licenses/by-nc-nd/4.0/).

¹D.Y., J.H., and X.J. contributed equally to this work.

²To whom correspondence may be addressed. Email: jing.hu1@uq.net.au, zky@xzhmu.edu.cn, or jumingyan@xzhmu.edu.cn.

This article contains supporting information online at <https://www.pnas.org/lookup/suppl/doi:10.1073/pnas.2302126120/-/DCSupplemental>.

Published November 15, 2023.

Results

Blockade of NMDAR by MK-801 Alters Bone Marrow-Derived Macrophage Phenotypes and Functions. We first determined the expression of NMDAR on macrophages in an in vitro tumor setting. The NMDAR subunit NR1 was detected on bone marrow-derived macrophages (BMDMs) and expression was upregulated when cocultured with mouse Hepa1-6BL hepatocellular tumor cells, or treated with tumor cell-conditioned media (TCM) (Fig. 1 A–C). NMDAR subunit NR2B was detected, but not upregulated by TCM (SI Appendix, Fig. S1 A and B). Other NR2 subunits were hardly detectable on macrophages (SI Appendix, Fig. S1A).

To explore the underlying regulatory effects of NMDAR, we performed RNA-seq on BMDMs treated with MK-801. This analysis identified a total of 3,326 differentially expressed genes (DEGs), of which 1,522 were up-regulated and 1,804 were down-regulated after MK-801 treatment (Fig. 1D). Most of the downregulated genes were associated with an M2 macrophage phenotype (e.g., *Arginase 1* (*Arg1*), *Chil3*, *S100a8*, *S100a9*, *Il10*, *Lcn2*, *Cd163*, Fig. 1E). Among the total 3326 DEGs, 264 genes were immune-related (SI Appendix, Fig. S1C). These findings for selected genes were also confirmed by using qPCR (Fig. 1F). Kyoto Encyclopedia of Genes and Genomes

(KEGG) pathway enrichment analysis identified many pathways potentially affected by MK-801 treatment of macrophages, including positive regulation of cytokine production and cytokine-cytokine receptor interaction and chemokine signaling pathways (Fig. 1G).

Co-stimulatory molecules expressed by macrophages such as CD80 and CD86 are crucial for T cell activation. MK-801 treatment significantly upregulated the expression of these co-stimulatory molecules on BMDMs when cocultured with Hepa1-6BL cells (Fig. 1 H and I). Next, we examined the effects of NMDAR antagonist treatment of macrophages on T cell proliferation. Compared with controls, MK-801 treatment of macrophages significantly promoted T cell proliferation and release of IFN γ (Fig. 1 J and K). Additionally, treatment with MK-801 augmented macrophage phagocytosis of apoptotic Hepa1-6BL cells (Fig. 1L). These results indicate that blocking NMDAR may drive macrophage polarization to an M1-like phenotype.

MK-801 Treatment Enhances Immune-Mediated Tumor Control in Preclinical Tumor Models. Several studies suggested that NMDAR might directly regulate tumor cell proliferation and invasiveness (16, 17). To understand the impact of NMDAR on tumor progression in vivo, the syngeneic liver tumor and fibrosarcoma models were established by subcutaneously inoculating Hepa1-6BL

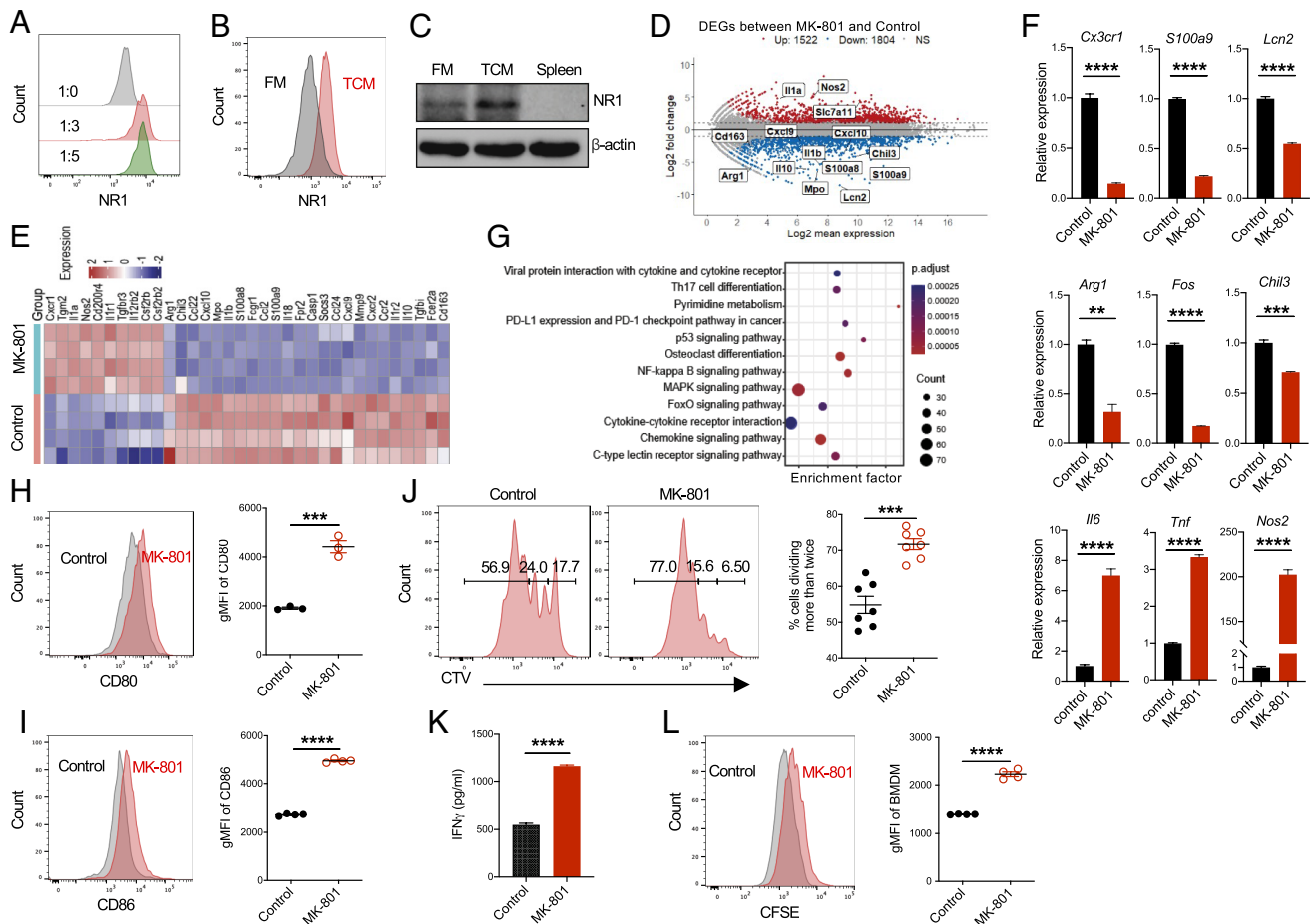


Fig. 1. MK-801 treatment alters the phenotype and function of macrophages. (A–C) NMDAR subunit NR1 expression in BMDMs cultured with (A) Hepa1-6BL cells at the indicated ratio, (B) fresh culture media (FM), or Hepa1-6BL tumor cell conditioned media (TCM) for 24 h determined by flow cytometry and (C) western blot. (D–G) DEGs and signaling pathway analyses of BMDMs treated with 300 μ M MK-801. (D) MA plot and (E) heatmap showing fold-change of DEGs of control versus MK-801 treatment. (F) Verification of the DEGs by qPCR in (E). (G) The bubble chart shows the signaling pathways. (H and I) Expression of CD80 and CD86 in BMDMs cocultured with Hepa1-6BL cells at the ratio of 1:1 in the presence or absence of 300 μ M MK-801 for 24 h. (J) The proliferation of OT1 CD8⁺ T cells after coculture with SIINFEKL-pulsed BMDMs. BMDM cells cocultured with Hepa1-6BL cells at the ratio of 1:1 in the presence or absence of 300 μ M MK-801 for 24 h. The percentage of T cells dividing more than twice was plotted. (K) The level of IFN γ in the cell culture supernatant from (J). (L) The phagocytic capacity of BMDMs against tumor cells. The data show the mean value \pm SEM. Experiments were performed twice, except for mRNA sequencing. Each dot represents a sample in the dot plots. Significant differences between groups as indicated by crossbars were determined using a Mann-Whitney test (F and H–L). ** $P < 0.01$, *** $P < 0.001$, **** $P < 0.0001$.

and MCA205 tumor cells in C57BL/6 wild-type (WT) mice respectively. Treatment with MK-801 significantly suppressed subcutaneous tumor growth, with a significant reduction of tumor mass (Fig. 2 A–D and *SI Appendix*, Fig. S2A). Moreover, treatment with MK-801 significantly reduced the numbers and sizes of the orthotopic liver tumor nodules in mice transplanted with Hepa1-6BL by high-pressure flux, leading to prolonged survival (Fig. 2 E and F). The potential adverse outcomes of MK-801 treatment in mice were assessed by monitoring body weight and analyzing liver tissue histology in tumor-bearing mice. There was no change in the body weight or histology of tumor-adjacent liver tissue in mice (*SI Appendix*, Fig. S2 B and C), indicating that MK-801 was tolerable and had no obvious side effects.

No significant changes in Hepa1-6BL and MCA205 tumor cell proliferation or apoptosis were observed upon MK-801 treatment (Fig. 2 G–I). Thus, we hypothesized that MK-801 might predominantly act on non-tumor cells to mediate tumor suppression. CD8⁺ T cells and NK cells are the major cytotoxic immune cells for tumor

control. MK-801 treatment failed to suppress Hepa1-6BL tumor growth in mice treated with antibodies that depleted CD8⁺ T cells or NK cells (Fig. 2 J and K), indicating that CD8⁺ T cells and NK cells were required for anti-tumor effects by MK-801. Notably, the expression of NMDAR was detectable on TAMs, but not on other tumor-infiltrating immune subsets (*SI Appendix*, Fig. S2D). These raise a possibility that MK-801 acted primarily on TAMs. Indeed, the anti-tumor effects of MK-801 treatment were markedly diminished in mice treated with clodronate liposome that depleted phagocytotic cells (Fig. 2 L and M). Together, these results indicate that treatment with MK-801 augments anti-tumor immunity by acting on TAMs.

MK-801 Treatment Increased the Effector Function of Tumor-Infiltrating Lymphocytes. To better understand the impact of MK-801 treatment on tumor-infiltrating immune cells, single-cell RNA sequencing was performed. Tumor-infiltrating CD45.2⁺ cells were assigned to 13 clusters (Fig. 3A), based on marker gene

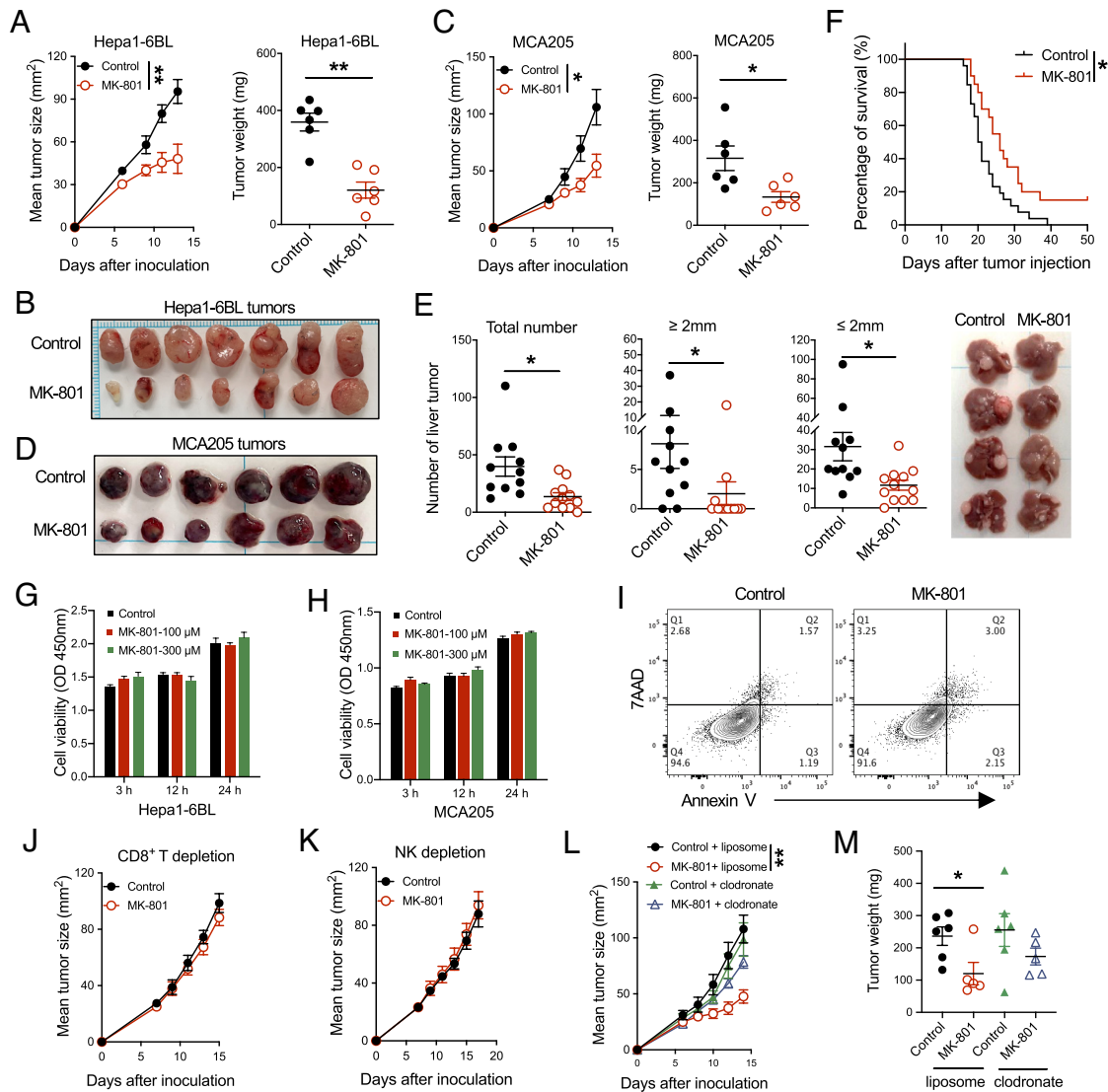


Fig. 2. MK-801 treatment suppressed tumor progression and prolonged mouse survival. (A–D) The effect of MK-801 treatment on the growth of Hepa1-6BL and MCA205 in C57BL/6 WT mice (6 to 7 mice/group) and representative tumor pictures. (E) The quantification of Hepa1-6BL liver tumors (Left) and representative images (Right) and (F) survival of C57BL/6 WT mice (10 to 15 mice/group) bearing Hepa1-6BL liver tumors. (G–I) Cell viability of (G) Hepa1-6BL cells, (H) MCA205 cells treated with MK-801 as indicated, and (I) cell apoptosis of Hepa1-6BL cells treated with 300 μM MK-801 for 48 h. (J–M) The effect of MK-801 treatment on Hepa1-6BL tumor growth in WT mice (9 to 12 mice/group) depleted of (J) CD8⁺ T cells, (K) NK cells, (L and M) macrophages. The details of mouse treatments were described in the methods of *SI Appendix*. The data show the mean value ± SEM. Experiments were performed twice independently with (A) three times, whereas (E and F) were pooled from two independent experiments. Each dot represents a mouse sample in the dot plots. Significant differences between groups were determined using a Mann-Whitney test (A, C, E, and J–M), or a log-rank Mantel-Cox test for F. **P* < 0.05; ***P* < 0.01.

expression of immune populations (Fig. 3B and *SI Appendix, Figs. S3 and S4*). Macrophages and monocytes were the predominant TILs, accounting for 50% and 25% of total TILs, respectively (Fig. 3C). MK-801 treatment slightly reduced the frequency of macrophages

and monocytes, while it increased CD4⁺ and CD8⁺ T cell frequencies (Fig. 3C). Neutrophils and pDCs frequencies were also increased after MK-801 treatment, while NK cell frequencies remained unchanged (Fig. 3C).

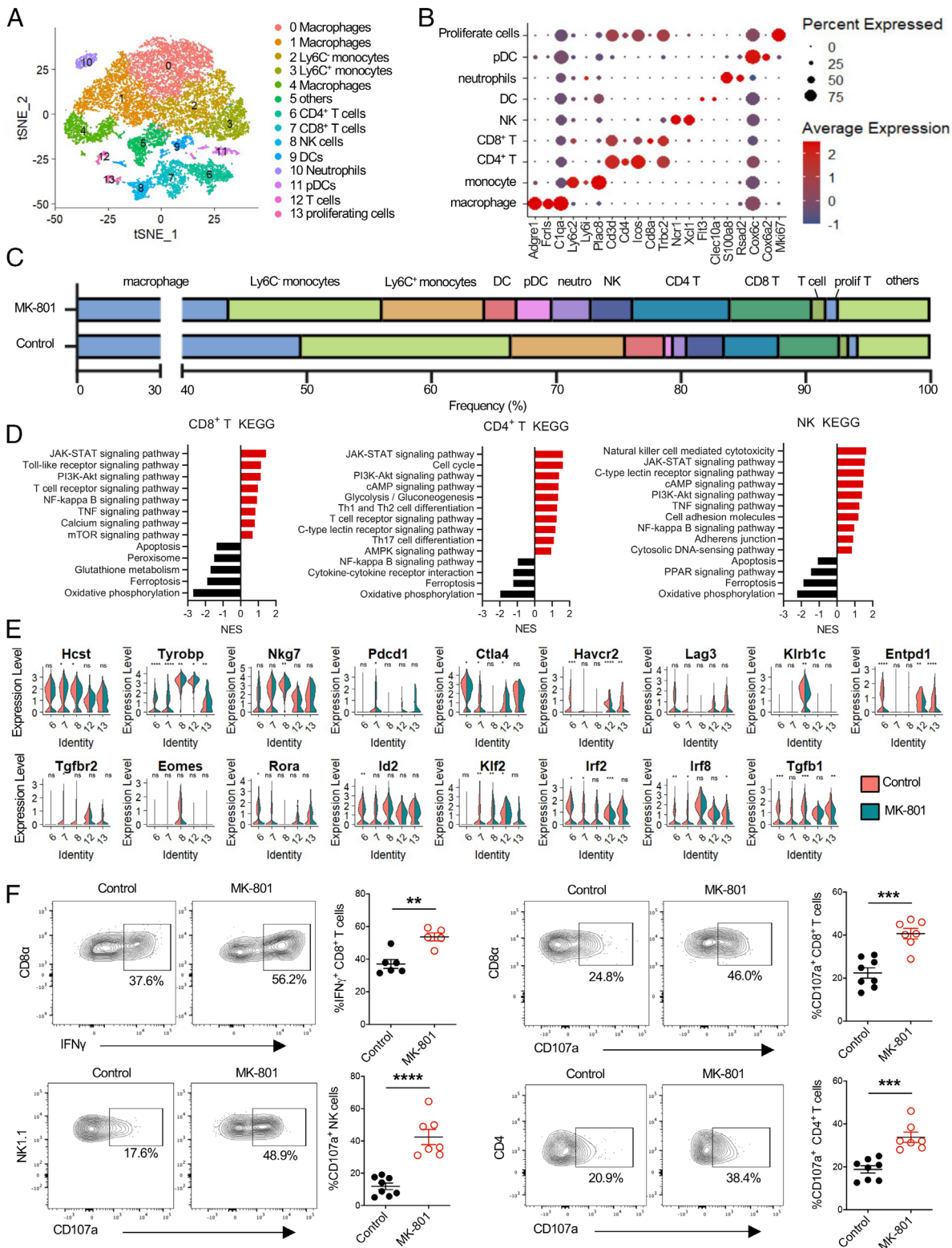


Fig. 3. MK-801 treatment increased the function of tumor-infiltrating cytotoxic lymphocytes. (A) tSNE analysis of CD45.2⁺ cells from Hepa1-6BL tumors. (B) Expression of the marker genes for each cluster for cell type identification. (C) The proportion of different cell subpopulations among tumor-infiltrating CD45.2⁺ cells shown in (A) on TILs of control and MK-801-treated Hepa1-6BL-bearing WT mice. (D) Enriched KEGG pathways of tumor-infiltrating CD8⁺ T, CD4⁺ T, and NK cells after MK-801 treatment. (E) Violin diagrams show DEGs in specific cell clusters shown in (A) on TILs of control and MK-801-treated Hepa1-6BL-bearing WT mice. (F) Representative plots and the quantification of IFN γ and CD107a expression in tumor-infiltrating CD8⁺ T, NK, and CD4⁺ T cells and from Hepa1-6BL tumors. Each dot represents a mouse sample in the dot plots. Representative dot plot and data presented as mean \pm SEM. Experiments were performed twice. Significant differences between groups as indicated by crossbars were determined by a Mann-Whitney test. ***P* < 0.01; ****P* < 0.001; *****P* < 0.0001.

Gene set enrichment analysis (GSEA) in NK, CD4⁺ and CD8⁺ T cells indicated that KEGG pathways representing positive regulation of cell proliferation, cell activation and cell-mediated cytotoxicity were enriched and upregulated, while cell apoptosis, metabolism such as OXPHOS and ferroptosis pathways were downregulated by MK-801 treatment (Fig. 3D). We next analyzed the expression of activation markers and immune checkpoint molecules on TILs and found that levels of the activation markers *Hcst*, *Tyrbp*, *Nkg7*, and *Pdcd1* were upregulated by MK-801 (Fig. 3E). The expression levels of inhibitory checkpoints such as *Havcr2* (Tim3), *Lag3* and *Entpd1* (CD39) in T cells was decreased after MK-801 treatment, as well as transcription factors negatively associated with anti-tumor functions (such as *Irf8*, etc.) (Fig. 3E). TGFβ1 production and TGFβ receptor II expression were dramatically downregulated by T and NK cells after MK-801 treatment (Fig. 3E).

To further validate enhanced lymphocyte activities following MK-801 treatment, we investigated IFNγ production and degranulation of cytotoxic molecules by flow cytometry. The proportion of IFNγ-producing CD8⁺ T cells was significantly increased by MK-801 treatment. The frequencies of NK, CD4⁺, and CD8⁺ T cells degranulating, as indicated by CD107a-expression, was significantly upregulated by MK-801 treatment (Fig. 3F). Of note, MK-801 treatment showed only modest effects on lymphocytes in the draining lymph nodes and spleen (SI Appendix, Figs. S5 and S6), suggesting that it predominantly altered effector lymphocytes in the TME.

MK-801 Treatment Altered the Gene Expression Profile in TAMs. Biological processes including response to interferons, cell differentiation, immune response to tumor cells, and KEGG pathways associated with promoting T cell activation, including antigen processing and Fc gamma receptor-mediated phagocytosis were upregulated in all macrophages after MK-801 treatment. Similarly, glycolysis was upregulated upon MK-801 treatment, while OXPHOS was downregulated (Fig. 4A). NMDAR blockade altered many pathways involved in the functions of two distinct Ly6C⁺ and Ly6C⁻ monocyte subtypes (SI Appendix, Fig. S7A). Interestingly, NMDAR activity and calcium ion transmembrane transport were enriched in cluster 4 macrophages specifically. GSEA analysis comparing MK-801 versus control samples showed core genes involved in the function and metabolism of macrophages, such as phagocytosis, cellular energy metabolism, type I IFN production, and IFNγ response (Fig. 4B).

Further analysis of the transcriptome of individual TAMs indicated that MK-801 treatment led to phenotypic alterations, including the downregulation of inhibitory immune checkpoints (*Havcr2*, *Entpd1*, *Cd274*, *Lilrb4a*, etc.), and molecules associated with M2 macrophages (*Mrc1*, *Arg1*, *Fn1*, etc.). The expression of transcription factors involved in M2 polarization was significantly decreased by MK-801, such as *Stat3*, *Irf8*, and *Hif1a*. Likewise, expression of angiogenic factors such as VEGFa and immunosuppressive molecules such as TGFβ1 were decreased, as was the chemokine *Cxcl10* (Fig. 4C). The decrease in VEGFa levels in MK-801-treated tumor tissue was verified by immunohistochemistry (SI Appendix, Fig. S7B) and was also reflected by fewer blood vessels, indicated by CD31 staining (SI Appendix, Fig. S7C). Our ex vivo experiments showed that upon MK-801 treatment, the expression of CD80 and CD86 was also significantly upregulated on Hepa1-6BL-infiltrating TAMs (SI Appendix, Fig. S7D and E). When cocultured with TAMs sorted from MK-801-treated tumors compared with control counterparts, CD8⁺ T cells proliferated greater, displayed stronger killing effect against tumor cells and produced more cytotoxic cytokines (Fig. 4D–F). Overall, these results indicate that MK-801 treatment decreased the immune suppressive phenotype and function of TAMs.

NMDAR Regulated Calcium Influx and Metabolism of Macrophages.

Given that NMDAR is a calcium channel, we investigated the effect of tumor cell supernatant on the calcium levels in BMDMs. Similar to the effects of glutamate and NMDA, Hepa1-6BL TCM substantially increased the cytosolic calcium levels (Fig. 5A). NMDA failed to induce calcium influx when calcium was chelated in the media (SI Appendix, Fig. S8A). The high Fluo-4 signal was also observed in the presence of 2-Aminoethoxydiphenylborane (2-APB) that blocks calcium release from the endoplasmic reticulum, supporting that TCM induced calcium influx. In contrast, MK-801 and MEM substantially inhibited TCM-mediated calcium influx. Similar to NMDA, the effect of Hepa1-6BL TCM on calcium influx was suppressed in MK-801 and MEM pre-treated macrophages (Fig. 5A). Consequently, the activation of NMDAR downstream kinase CaMKII and ERK1/2 as well as transcriptional factor CREB in macrophages by TCM was counteracted by MK-801 (Fig. 5B). The presence of ERK1/2 inhibitor diminished the effect of MK-801 on the phosphorylation of CREB (Fig. 5C). The level of glutamate in TCM was substantially higher than that in BMDM-conditioned media (BCM) and fresh media (FM) (Fig. 5D). These results indicate tumor cell-released glutamate might activate NMDAR and downstream pathways.

It is known that calcium influx induces the generation of reactive oxygen species (ROS). Therefore, the effect of NMDAR antagonists on ROS production was determined. MK-801 and MEM significantly decreased ROS levels in macrophages cultured in TCM (Fig. 5E and SI Appendix, Fig. S8B). Glutathione is a major antioxidant in cells. However, no significant change in the level of glutathione was observed after MK-801 and MEM treatment (SI Appendix, Fig. S8C). The majority of intracellular ROS is derived from superoxide radicals, which are mainly generated by mitochondrial metabolism, peroxisomes, and NADPH oxidases (NOXs) (18). The mRNA levels of *Nox1* and *Mpo* were significantly decreased after NMDAR blockade, as well as the levels of the mitochondrial NADH dehydrogenase complex components *mt-Nd1* and *mt-Nd3* and cytochrome C oxidases *mt-Co2* and *mt-Co3* (Fig. 5F), suggesting a role for these ROS pathways in the intracellular changes caused by MK-801 and MEM treatment.

Intracellular ROS can cause lipid peroxidation and lipid membrane damage (18). TCM significantly increased lipid peroxidation levels compared with fresh media, while MK-801 and MEM suppressed the effect of TCM (Fig. 5G). Correspondingly, the NMDAR antagonists also diminished the damage to mitochondrial structure induced by TCM (Fig. 5H). The ratio of intracellular ADP/ATP was measured to evaluate a potential shift in intracellular energy metabolism. In line with our previous observations, TCM decreased the ratio of ADP/ATP compared with fresh media. Blocking NMDAR with MK-801 and MEM significantly increased the ratio of ADP/ATP (Fig. 5I). Similar to TAMs (Fig. 4A and B), BMDMs treated with MK-801 also showed reduced OXPHOS according to GSEA-KEGG pathway analysis (Fig. 5J). To confirm a potential change in macrophage energy metabolism, we performed Seahorse experiments to determine the oxygen consumption rate (OCR) as a measure of OXPHOS. BMDMs treated with TCM had higher maximal OCRs, indicating strong OXPHOS capacity. As expected, NMDAR antagonist-treated BMDMs displayed lower maximal respiration and spare respiration capacity in the presence of TCM, but ATP production in mitochondria was unchanged (Fig. 5K).

Mg²⁺ Decreased the Immunosuppression of Macrophages via NMDAR. Some studies reported that Mg²⁺ in cell culture media promoted the maturation of monocytes into adhering macrophages showing altered cytokine production profiles (19, 20). Mg²⁺ is a natural channel blocker of NMDAR. Our results demonstrated

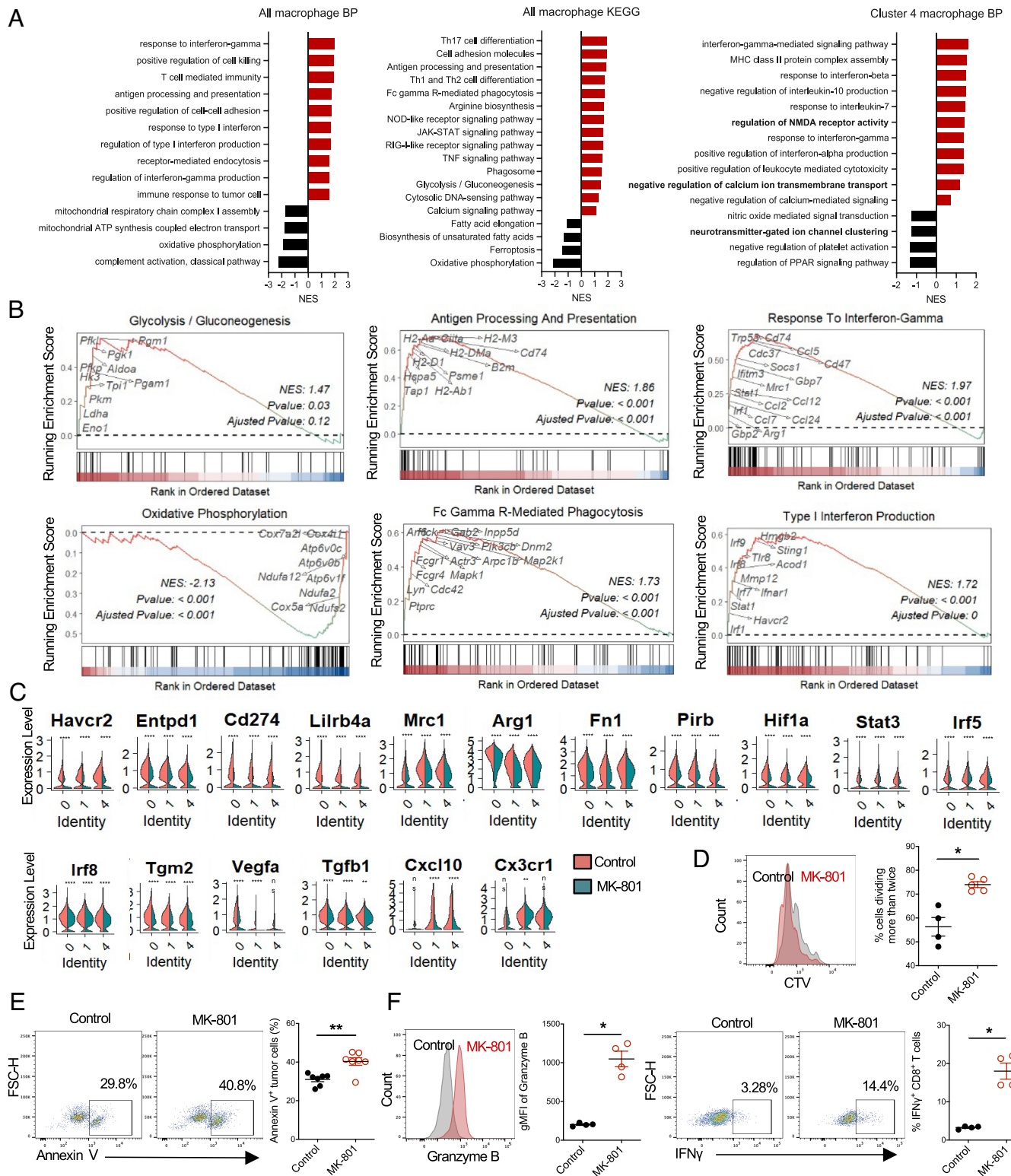


Fig. 4. MK-801 treatment altered the gene expression profile and function of TAMs. (A) GSEA-KEGG and Gene Ontology (GO) analysis of all macrophage clusters and cluster 4 macrophages from control tumors and MK-801-treated tumors. Potential functions and pathways are listed on the y axis. Pathway enrichment is shown as the normalized enrichment scores (NES) adjusted for multiple comparisons. (B) GSEA analysis of core gene variation involved in the function and metabolisms of macrophages. Statistical testing was performed by permutation test. The *P*-values were corrected with Benjamini-Hochberg adjustment. (C) Violin plots indicating the expression of selected genes in each macrophage cluster present in control and MK-801-treated tumors. The statistical difference was calculated by Student's *t* test. (D–F) The effects of MK-801 on the immunosuppressive function of TAMs against CD8⁺ T cells as described in the method. (D) CD8⁺ T cell proliferation, (E) the apoptosis of Hepa1-6BL to reflect the killing ability of CD8⁺ T cells, (F) Granzyme B and IFN γ expression in CD8⁺ T cells. Each dot represents a sample in the dot plots. Representative dot plot and data presented as mean \pm SEM. Experiments were performed twice. Significant differences between groups as indicated by crossbars were determined by a Mann-Whitney test. **P* < 0.05; ***P* < 0.01, ****P* < 0.001; *****P* < 0.0001.

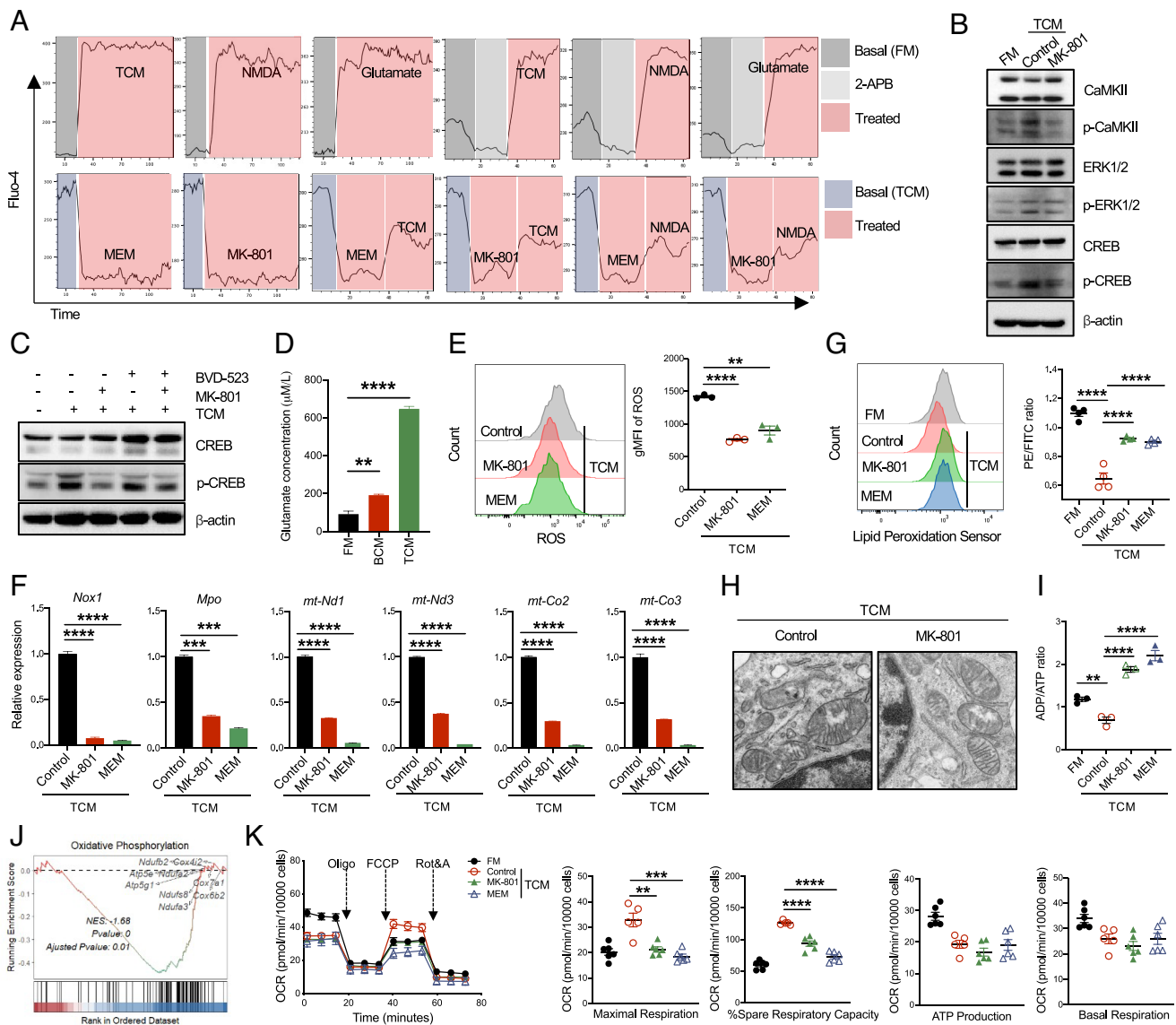


Fig. 5. NMDAR regulated Ca^{2+} influx, ROS production, and the function of mitochondria in macrophages. (A) Ca^{2+} influx in BMDMs. Average fluorescence ratio over time of BMDMs exposed sequentially to FM, Hepa1-6BL TCM, glutamate (1 mM), NMDA (300 μM), MEM (300 μM), MK-801 (300 μM), 2-APB (10 μM) as indicated, by detecting the Fluo-4 fluorescence intensity using flow cytometry. The Fluo-4 fluorescence intensity over time was analyzed using FlowJo software kinetic module to reflect the level of calcium in the cell cytosol. (B and C) The level of total protein and phosphorylation of CaMKII, ERK1/2, and CREB in BMDMs after the indicated treatment by western blot. (D) Glutamate levels in supernatants of fresh cell culture media (FM), or BCM, and Hepa1-6BL tumor cell conditioned media (TCM). (E–G) Quantization of ROS levels (E), relative mRNA level of genes involved in ROS production (F), and quantization of lipid peroxidation (G) in BMDMs after the indicated treatments by flow cytometry. (H) Representative electron microscope images of mitochondrial morphology of BMDMs. (I) The ratio of ADP to ATP in BMDMs after the indicated treatment. (J) The enrichment plot of genes involved in OXPHOS in BMDMs after MK-801 treatment. (K) The effect of NMDAR antagonists on BMDM OXPHOS as described in the *SI Appendix, Methods*. The data is presented as mean \pm SEM. Each dot represents a sample in the dot plots. Experiments were performed twice independently with (A) four times. Significant differences between groups as indicated by crossbars were determined by a Mann-Whitney test. $**P < 0.01$; $***P < 0.001$; $****P < 0.0001$.

that Mg^{2+} inhibited calcium influx in macrophages induced by TCM. Mg^{2+} pretreatment had a similar suppressive effect to MK-801 on calcium influx (*SI Appendix, Fig. S9A*). Similarly, pretreatment of macrophages with MK-801 and MEM made Mg^{2+} incapable of suppressing calcium influx further (*SI Appendix, Fig. S9A*). In line with a previous study (19), ROS levels were significantly decreased by Mg^{2+} in macrophages cultured in TCM. In the presence of Mg^{2+} , MK-801 treatment failed to decrease ROS production further (*SI Appendix, Fig. S9B*). Treatment with Mg^{2+} dramatically upregulated mRNA levels of *Nos2*, *Il6*, and *Tnf* in macrophages (*SI Appendix, Fig. S9C*). Of interest, co-administration of MK-801 and Mg^{2+} had a similar effect as single agent treatment on the expression of pro-inflammatory cytokines (*SI Appendix, Fig. S9C*). These results indicate that the effect

of magnesium on macrophages was associated with NMDAR activity. The expressions of Arginase 1, PD-L1 and VEGFa were substantially downregulated by MK-801, MEM and Mg^{2+} in TCM-treated macrophages (*SI Appendix, Fig. S9D*).

Similar to MK-801, Mg^{2+} treatment decreased the suppressive effect of TCM-cultured macrophages on OT1 T cell proliferation in the presence of OVA antigen (*SI Appendix, Fig. S9E*). A similar coculture experiment was performed using anti-CD3 antibody-stimulated CD8^+ T cells and TCM-treated macrophages. Similar to MK-801 and MEM treatment, Mg^{2+} increased T cell proliferation following coculture with TCM-treated macrophages in the presence of anti-CD3 antibody (*SI Appendix, Fig. S9F*). These results indicate that Mg^{2+} diminished the suppression of TCM-treated macrophages on T cell proliferation via blocking NMDAR on macrophages.

Blocking NMDAR Improved the Efficacy of Anti-PD-1 Treatment.

To further validate the therapeutic potential of NMDAR antagonists, we tested the antitumor effect of clinical drugs that target NMDAR including MEM, ifenprodil tartrate, and MgCl₂. Administrating MEM in drinking water significantly suppressed Hepa1-6BL tumor growth in mice (Fig. 6A and B). Similar to the effect of MK-801 on TAM, MEM treatment also decreased the immunosuppressive effect of TAM as indicated by the cocultured CD8⁺ T cell proliferation, killing ability, and cytokine production (SI Appendix, Fig. S10). Anti-tumor effects were also achieved by ifenprodil tartrate and MgCl₂ treatment (Fig. 6C).

Intriguingly, in response to treatment with MK-801, the frequency of PD-1 expressing tumor-infiltrating CD8⁺ T cells increased (Fig. 6D). Thus, we addressed whether treatment with MK-801 could improve the efficacy of anti-PD-1. In mice bearing Hepa1-6BL, 30% achieved tumor-free status in response to a single dose of anti-PD-1 treatment (Fig. 6E). Strikingly, the addition of NMDAR antagonists to anti-PD-1 treatment markedly improved tumor control with more than 65% of mice achieving complete rejection (Fig. 6E and F). Together, the findings indicate that targeting NMDAR to alter Ca²⁺ signaling pathways and metabolism is a potential approach to improve the efficacy of anti-PD-1 immunotherapy (Fig. 6G).

Discussion

In the current study, we revealed NMDAR as a regulator of macrophage functions in the TME and demonstrated that therapeutic

targeting of NMDAR with selective antagonists stimulated anti-tumor immunity. The combined effect of clinically used NMDAR antagonists such as MEM and ifenprodil tartrate with PD-1 antibody led to promising tumor rejection rates underscoring a translational potential.

Previous studies reported that tumor cells express NMDAR to promote proliferation, survival, and invasion, and proposed targeting NMDAR on tumor cells to control tumor progression, supported by findings in several xenograft tumor models in immune-deficient mice (16, 17, 21, 22). Our work explored the regulatory role of NMDAR in TAMs and highlighted anti-tumor mechanisms of NMDAR antagonists on immune cells. Here, we demonstrate that blocking NMDAR is a promising immunotherapeutic strategy, and different selective antagonists against NMDAR effectively suppressed tumor growth and prolonged survival in syngeneic mouse tumor models. Notably, MEM is used in clinics mainly to treat Alzheimer's disease. A recent phase 1 study reported the safety and maximum tolerated dose of combinations of MEM with temozolomide as post-irradiation adjuvant therapy for newly diagnosed glioblastoma (23). These clinical results support the feasibility of targeting NMDAR in cancer patients.

In the TME, macrophages can develop into immune suppressive phenotypes, driving tumor progression. An attractive immunotherapeutic approach has been to convert TAMs into tumoricidal macrophages, rather than depleting them (4). In our syngeneic murine tumor model, the depletion of macrophages did not affect tumor growth but abolished the tumor suppressive effect of

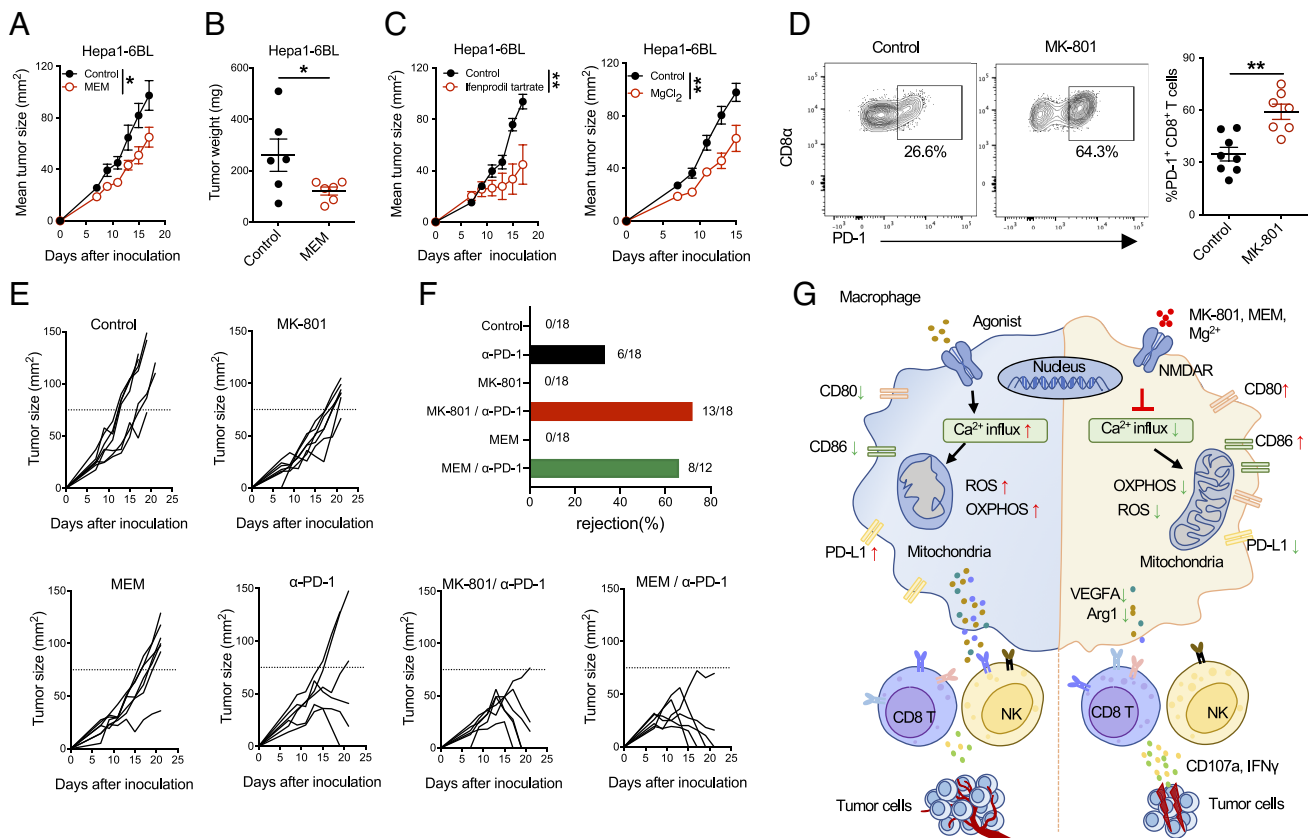


Fig. 6. Blocking NMDAR and PD-1 resulted in tumor rejection. (A–C) The effect of NMDAR antagonist Hepa1-6BL tumor growth. Tumor-bearing C57BL/6J WT mice (5 to 8 mice per group) were treated from day 5, daily with MEM (25 mg/kg, in drinking water), ifenprodil tartrate (20 mg/kg, i.p.) and MgCl₂ (50 μL of 3 mM intratumorally). The data show the mean tumor size (mm²) ± SEM. (D) Representative plots and the quantification of PD-1 in Hepa1-6BL tumor infiltrating CD8⁺ T cells by flow cytometry. Each dot represents a mouse sample in the dot plots. (E) The effect of NMDAR antagonist and anti-PD-1 antibody treatment (i.p. 100 μg/mouse on day 11), alone or in combination as indicated on the established Hepa1-6BL tumor growth in C57BL/6J WT (5 to 8 mice per group). Each growth curve represents a mouse tumor. (F) Statistics of tumor rejection rate in the groups as in (E). Data were pooled from two independent experiments. (G) Schematic for the mechanisms by blocked NMDAR in decreased the suppressive function of TAM and improved the function of cytotoxic lymphocytes in TME. Experiments were performed twice. Significant differences between groups as indicated by crossbars were determined using a Mann-Whitney test. **P* < 0.05; ***P* < 0.01.

MK-801. The immune suppressive function of TAMs in TME was suppressed by NMDAR antagonists. Our single-cell transcriptomic analysis and *in vitro* assays showed that blocking NMDAR was a potential strategy to reshape TAMs as shown by the downregulation of inhibitory molecules (TGF β , Arginase 1, CD39 and PD-L1, etc.) (4, 24, 25) and by upregulation of costimulatory molecule CD80 and CD86. The changes of these immune regulatory molecules in TAMs after NMDAR blocking together mediate the suppression of TAMs on the proliferation and function of T and NK cells in the TME.

It is reported that glutamate could be transported by a variety of transporters, such as the xCT channel that exports glutamate in exchange for cystine to maintain redox homeostasis in tumor cells (26). Indeed, a high level of glutamate was detected in TCM. We observed that similar to glutamate and NMDA treatment, TCM-triggered influx of calcium in macrophages was prevented by NMDAR antagonists. Therefore, it is reasonable to propose that macrophages are sculpted into immunosuppressive cells through NMDAR activation by tumor cell-released NMDAR agonists. Tumor cell xCT supports tumor cell survival against oxidative stress, but also suppresses antitumor immunity (27). Our finding suggests that tumor cell-glutamate activates NMDAR on TAM and promotes the immunosuppressive function of TAMs and provides a possible mechanism for tumor cell xCT to hamper immune responses.

Although some tumor cells can secrete a high level of glutamate which can activate NMDAR in the TME, glutamate from other cells may also contribute to NMDAR activation. Our data demonstrated that macrophages secreted glutamate but much lower than tumor cells, indicating macrophage-secreted glutamate might form a weak constitutive NMDAR activation in an autocrine manner. Of note, glutamate might not be the only NMDAR ligand in the TCM because other NMDAR modulators/co-agonists such as polyamine, glycine, and zinc ion may also be present (28).

NMDAR-calcium is associated with the CaMKII and ERK pathways that regulate CREB activation in neurons (29, 30). Both ERK signaling and CREB activation are critical for M2 macrophage polarization (31, 32). Indeed, our data shows that CaMKII/ERK/CREB is the downstream pathway of NMDAR in TAMs. NMDAR-calcium regulates many signaling pathways, other pathways may also be involved. The downstream signaling patterns of neuron synaptic and extrasynaptic NMDAR are different, generating different biological effects (30). In neurons, synaptic NMDAR activates CREB through CaMKII and ERK1/2 and promotes cell survival, while extrasynaptic NMDAR activation suppresses CREB activity and causes mitochondrial damage inducing cell death. In our study, NMDAR-mediated signaling in macrophages resembles the synaptic pattern as indicated by the ERK and CREB phosphorylation. Recently, it has been reported that the TRPM4 cation channel played an important role in mediating extrasynaptic NMDAR signaling (33). Therefore, it might be of help to determine the interaction of TRPM4 and NMDAR for revealing the existence of extrasynaptic NMDAR signaling in TAMs.

In our tumor setting, we observed alterations in the metabolism of macrophages. The influx of calcium increases OXPHOS. Indeed, our *in vivo* and *in vitro* data demonstrate that blocking NMDAR decreased OXPHOS in macrophages. ADP/ATP homeostasis has a profound effect on macrophages (34). TCM dampened the ADP/ATP ratio compared with fresh media, which was converted by blocking NMDAR. Our data also showed that NMDAR blockade suppressed the production and cytotoxic effects of ROS, including lipid peroxidation and mitochondria structure damage. In addition, ROS could modulate macrophage immunosuppressive phenotype through the up-regulation of PD-L1 (35). This is in line with our

observation that NMDAR blockade downregulated both ROS and PD-L1 expression in TAMs.

The participation of Mg²⁺ in various cellular processes and its immune regulatory role has been reported. Mg²⁺ regulates cytokine production and ROS production in macrophages (19, 36, 37). It was proposed that Mg²⁺ acted intracellularly because Mg²⁺ exposure rapidly increased the intracellular Mg²⁺ content, and decreased pro-inflammatory cytokine production (20). Our study revealed that NMDAR is a target in macrophages for Mg²⁺ in tumor settings. To the best of our knowledge, the regulatory effect of Mg²⁺ on macrophages via NMDAR has not been investigated in a tumor setting. Systematic administration of Mg²⁺ is not practical in the clinical setting for tumor treatment. A nanoparticle-mediated drug delivery strategy could tackle the issue (19). Systemic administration of liposomal encapsulated Mg²⁺ suppressed tumor growth with a similar effect as intratumoral Mg²⁺ treatment in pre-immunized, rather than in non-immunized mice. The authors showed that Mg²⁺ played an important role in memory T cell activation via binding to adhesion molecule LFA1 on T cells in the immune synapse, but the effect of Mg²⁺ on TAMs was not investigated in the study (38). We envisage that proper on-target administration of Mg²⁺ will regulate both T cells and macrophages in the TME.

Neural-immune cross-talk in the TME occurs and profoundly influences tumor progression (39, 40). A range of neurotransmitters can affect anti-tumor immunity or immunotherapeutic effects (39–42). Glutamate could be converted into gamma-aminobutyric acid (GABA) by glutamic acid decarboxylases (GAD1/2) (43). Autocrine GABA signaling through the GABAB receptor in colon cancer cells promotes cancer cell proliferation, while reducing expression and secretion of the CCL4 and CCL5 chemokines by colon cancer cells, thereby inhibiting T lymphocytes and dendritic cells infiltrating into tumors (43). Furthermore, binding of B cell-derived GABA to GABAA receptors on T cells suppressed cytotoxic T cell responses and promoted an immune-suppressive state in TAMs (44). In addition, platelet-derived peripheral serotonin upregulates tumor PD-1 expression and suppresses T cell cytotoxic activity (45). It has been proposed that neuronal regulatory pathways co-opted in cancer cells are implicated in facilitating the acquisition of hallmark capabilities and associated parameters such as avoiding immune destruction (39, 40).

NMDAR is an important neuron transmitter receptor, with high expression on nerve cells. Recently, the infiltration of nerve cells in tumors such as breast cancer has been reported to be associated with cancer outcomes (46). Synaptic proximity enables NMDAR signaling to promote breast cancer to brain metastasis (46). Bupivacaine is a local anesthetic used to prevent pain by the blockage of sodium ion channels including NMDAR. Bupivacaine nanoparticles effectively suppressed mouse breast cancer progression and metastases by targeting neurons in the TME (47). In our study, NMDAR signaling in macrophages was activated in the TME and promoted the immunosuppressive function of macrophages, leading to tumor immune evasion. Although our data show that NMDAR blockade reduced the immunosuppressive function of TAMs and suppressed tumor progression in the mouse tumor models, the presence of neurons in our tumor models remains to be investigated, especially the involvement of the neuronal system that is targeted by the NMDAR antagonists.

In summary, our study demonstrated the expression of neural transmitter receptor NMDAR on macrophages in the TME and uncovered the unknown role of NMDAR in regulating macrophage function and effects on anti-tumor immune responses in the used tumor models. However, the generality of NMDAR signaling in TAMs in other tumor types still needs to be verified. Overall, our

results identified NMDAR agonists as a promising class of therapeutics to improve the efficacy of cancer immunotherapy.

Materials and Methods

Detailed descriptions of all materials and reagents are listed in *SI Appendix, Tables S1–S4*. The methods including cell culture, establishment of tumor models, mouse treatments, tumor-infiltrating immune cell analysis and sorting by using flow cytometry, and the assays to determine the function of macrophages, calcium flux, OXPHOS, ROS production, single-cell RNA sequencing and analysis, and statistics can be found in *SI Appendix*.

All animal experimental procedures were strictly performed according to the Guidelines for Animal Experiments of Xuzhou Medical University and the National Guide for the Care and Use of Laboratory Animals. All experiments were approved by the Xuzhou University Animal Ethics Committee (202209S041).

Data, Materials, and Software Availability. Source data are provided with this paper. RNA sequencing data for Figs. 1d, 1e, and 1g from BMDMs is available, and Single-cell RNA sequencing data for tumors associated with Figs. 3b to 3e and 4a, 4b, 4c is accessible to the public. All source data have been submitted to the Figshare database (<https://doi.org/10.6084/m9.figshare.24447394>) (48). All study data are included in the article and/or *SI Appendix*.

ACKNOWLEDGMENTS. We thank Hui Hua, Xiangyang Li, Wangpeng Chen. We also like to thank Yan Li, Michele W. L. Teng, Jing Yang, and Hui Wang for their intellectual input and helpful discussions. J.Y. is funded by the National

Natural Science Foundation of China (NSFC) for Young Scholars (82103445), Jiangsu Province NSFC for Young Scholars (BK20210898), Starting Foundation for Talents of Xuzhou Medical University (RC20552063), Innovation Program for Young Scholar of Xuzhou Medical University (KY14012202), Specially Appointed Professor Program of Jiangsu Province of China, Open Competition Grant of Xuzhou Medical University. J.H. by the NSFC for Young Scholars (82203541) and Xuzhou Science and Technology Foundation for Young Scholars (KC21059). E.M.P. is funded by the St. Anna Children's Cancer Research Institute (Vienna, Austria) and the Austrian Science Fund (FWF P32001-B and P34832-B).

Author affiliations: ^aDepartment of Pathogen Biology and Immunology, Jiangsu Key Laboratory of Immunity and Metabolism, Jiangsu International Laboratory of Immunity and Metabolism, Xuzhou Medical University, Xuzhou, Jiangsu 221004, China; ^bDepartment of Bioinformatics, School of Life Sciences, Xuzhou Medical University, Xuzhou, Jiangsu 221004, China; ^cDepartment of Genetics, Xuzhou Engineering Research Center of Medical Genetics and Transformation, Xuzhou Medical University, Xuzhou, Jiangsu 221004, China; ^dSt. Anna Children's Cancer Research Institute, Medical University of Vienna, Vienna 1210, Austria; ^eJiangsu Province Key Laboratory in Anesthesiology, School of Anesthesiology, Xuzhou Medical University, Xuzhou, Jiangsu 221004, China; ^fDepartment of Pathogen Biology, Jiangsu Province Key Laboratory of Modern Pathogen Biology, Nanjing Medical University, Nanjing, Jiangsu 211166, China; ^gDepartment of Pulmonary Medicine, Shanghai Chest Hospital, School of Medicine, Shanghai Jiao Tong University, Shanghai 200240, China; ^hJiangsu Key Laboratory for Pharmacology and Safety Evaluation of Chinese Materia Medica, School of Pharmacy, Nanjing University of Chinese Medicine, Nanjing, Jiangsu 210023, China; ⁱDepartment of Biochemistry and Molecular Biology, School of Medicine and Holistic Integrative Medicine, Nanjing University of Chinese Medicine, Nanjing, Jiangsu 210023, China; ^jDepartment of Research and Development, OriCell Therapeutics Co. Ltd, Shanghai 200131, China; and ^kTranslational Oncology Discovery Group, QIMR Berghofer Medical Research Institute, Brisbane 4702, Australia

1. D. Hanahan, R. A. Weinberg, Hallmarks of cancer: The next generation. *Cell* **144**, 646–674 (2011).
2. D. Hanahan, Hallmarks of cancer: New dimensions. *Cancer Discov.* **12**, 31–46 (2022).
3. D. B. Johnson, C. A. Nebhan, J. J. Moslehi, J. M. Balko, Immune-checkpoint inhibitors: Long-term implications of toxicity. *Nat. Rev. Clin. Oncol.* **19**, 254–267 (2022).
4. A. Mantovani, P. Allavena, F. Marchesi, C. Garlanda, Macrophages as tools and targets in cancer therapy. *Nat. Rev. Drug Discov.* **21**, 799–820 (2022).
5. B. Ruffell, L. M. Coussens, Macrophages and therapeutic resistance in cancer. *Cancer Cell* **27**, 462–472 (2015).
6. R. Ostuni, F. Kratochvill, P. J. Murray, G. Natoli, Macrophages and cancer: From mechanisms to therapeutic implications. *Trends Immunol.* **36**, 229–239 (2015).
7. D. I. Gabrilovich, S. Ostrand-Rosenberg, V. Bronte, Coordinated regulation of myeloid cells by tumours. *Nat. Rev. Immunol.* **12**, 253–268 (2012).
8. A. Christofides *et al.*, The complex role of tumor-infiltrating macrophages. *Nat. Immunol.* **23**, 1148–1156 (2022).
9. J. N. Kew, J. A. Kemp, Ionotropic and metabotropic glutamate receptor structure and pharmacology. *Psychopharmacology (Berl)* **179**, 4–29 (2005).
10. F. J. van der Staay, K. Rutten, C. Erb, A. Blokland, Effects of the cognition impairer MK-801 on learning and memory in mice and rats. *Behav. Brain Res.* **220**, 215–229 (2011).
11. J. Folch *et al.*, Memantine for the treatment of dementia: A review on its current and future applications. *J. Alzheimers Dis.* **62**, 1223–1240 (2018).
12. S. Matsunaga, T. Kishi, N. Iwata, Memantine monotherapy for Alzheimer's disease: A systematic review and meta-analysis. *PLoS One* **10**, e0123289 (2015).
13. X. Song *et al.*, Mechanism of NMDA receptor channel block by MK-801 and memantine. *Nature* **556**, 515–519 (2018).
14. H. Cheng *et al.*, Over-activation of NMDA receptors promotes ABCA1 degradation and foam cell formation. *Biochim. Biophys. Acta Mol. Cell Biol. Lipids* **1865**, 158778 (2020).
15. W. Nowak *et al.*, Pro-inflammatory monocyte profile in patients with major depressive disorder and suicide behaviour and how ketamine induces anti-inflammatory M2 macrophages by NMDAR and mTOR. *EBioMedicine* **50**, 290–305 (2019).
16. L. Li, D. Hanahan, Hijacking the neuronal NMDAR signaling circuit to promote tumor growth and invasion. *Cell* **153**, 86–100 (2013).
17. L. Li *et al.*, GKAP acts as a genetic modulator of NMDAR signaling to govern invasive tumor growth. *Cancer Cell* **33**, 736–751.e5 (2018).
18. E. C. Cheung, K. H. Vousden, The role of ROS in tumour development and progression. *Nat. Rev. Cancer* **22**, 280–297 (2022).
19. W. Qiao *et al.*, TRPM7 kinase-mediated immunomodulation in macrophage plays a central role in magnesium ion-induced bone regeneration. *Nat. Commun.* **12**, 2885 (2021).
20. J. Sugimoto *et al.*, Magnesium decreases inflammatory cytokine production: A novel innate immunomodulatory mechanism. *J. Immunol.* **188**, 6338–6346 (2012).
21. G. Albayrak, E. Konac, A. U. Dikmen, C. Y. Bilen, Memantine induces apoptosis and inhibits cell cycle progression in LNCaP prostate cancer cells. *Hum. Exp. Toxicol.* **37**, 953–958 (2018).
22. W. G. North, F. Liu, L. Z. Lin, R. Tian, B. Akerman, NMDA receptors are important regulators of pancreatic cancer and are potential targets for treatment. *Clin. Pharmacol.* **9**, 79–86 (2017).
23. S. Maraka *et al.*, Phase 1 lead-in to a phase 2 factorial study of temozolomide plus memantine, mefloquine, and metformin as postirradiation adjuvant therapy for newly diagnosed glioblastoma. *Cancer* **125**, 424–433 (2019).
24. A. K. Moesta, X. Y. Li, M. J. Smyth, Targeting CD39 in cancer. *Nat. Rev. Immunol.* **20**, 739–755 (2020).
25. J. Yan *et al.*, Control of metastases via myeloid CD39 and NK cell effector function. *Cancer Immunol. Res.* **8**, 356–367 (2020).
26. J. K. M. Lim *et al.*, Cystine/glutamate antiporter xCT (SLC7A11) facilitates oncogenic RAS transformation by preserving intracellular redox balance. *Proc. Natl. Acad. Sci. U.S.A.* **116**, 9433–9442 (2019).
27. M. D. Arensman, X. S. Yang, D. M. Leahya, L. Toral-Barza, M. Mileski, Cystine–glutamate antiporter xCT deficiency suppresses tumor growth while preserving antitumor immunity. *Proc. Natl. Acad. Sci. U.S.A.* **116**, 10 (2018).
28. L. V. Kalia, S. K. Kalia, M. W. Salter, NMDA receptors in clinical neurology: Excitatory times ahead. *Lancet Neurol.* **7**, 742–755 (2008).
29. M. M. Stratton, Start spreading the news! CaMKII shares activity with naive molecules. *Proc. Natl. Acad. Sci. U.S.A.* **119**, e2216529119 (2022).
30. G. E. Hardingham, H. Bading, Synaptic versus extrasynaptic NMDA receptor signalling: Implications for neurodegenerative disorders. *Nat. Rev. Neurosci.* **11**, 682–696 (2010).
31. B. Luan *et al.*, CREB pathway links PGE2 signaling with macrophage polarization. *Proc. Natl. Acad. Sci. U.S.A.* **112**, 15642–15647 (2015).
32. L. He *et al.*, Global characterization of macrophage polarization mechanisms and identification of M2-type polarization inhibitors. *Cell Rep.* **37**, 109955 (2021).
33. J. Yan, C. P. Bengtson, B. Buchthal, A. M. Hagenston, H. Bading, Coupling of NMDA receptors and TRPM4 guides discovery of unconventional neuroprotectants. *Science* **370**, eaay3302 (2020).
34. W. Chen *et al.*, The phenotype of peritoneal mouse macrophages depends on the mitochondria and ATP/ADP homeostasis. *Cell Immunol.* **324**, 1–7 (2018).
35. C. Roux *et al.*, Reactive oxygen species modulate macrophage immunosuppressive phenotype through the up-regulation of PD-L1. *Proc. Natl. Acad. Sci. U.S.A.* **116**, 4326–4335 (2019).
36. A. Mazur *et al.*, Magnesium and the inflammatory response: Potential pathophysiological implications. *Arch. Biochem. Biophys.* **458**, 48–56 (2007).
37. R. Hang *et al.*, Exosomes derived from magnesium ion-stimulated macrophages inhibit angiogenesis. *Biomed. Mater.* **17**, 1748–605X (2022).
38. J. Lotscher *et al.*, Magnesium sensing via LFA-1 regulates CD8(+) T cell effector function. *Cell* **185**, 585–602.e29 (2022).
39. R. Mancusi, M. Monje, The neuroscience of cancer. *Nature* **618**, 467–479 (2023).
40. D. Hanahan, M. Monje, Cancer hallmarks intersect with neuroscience in the tumor microenvironment. *Cancer Cell* **41**, 573–580 (2023).
41. S. H. Jiang *et al.*, GABRP regulates chemokine signalling, macrophage recruitment and tumour progression in pancreatic cancer through tuning KCNN4-mediated Ca(2+) signalling in a GABA-independent manner. *Gut* **68**, 1994–2006 (2019).
42. G. Qiao, M. Chen, M. J. Bucsek, E. A. Repasky, B. L. Hylander, Adrenergic signaling: A targetable checkpoint limiting development of the antitumor immune response. *Front. Immunol.* **9**, 164 (2018).
43. D. Huang *et al.*, Cancer-cell-derived GABA promotes beta-catenin-mediated tumour growth and immunosuppression. *Nat. Cell Biol.* **24**, 230–241 (2022).
44. B. Zhang *et al.*, B cell-derived GABA elicits IL-10(+) macrophages to limit anti-tumour immunity. *Nature* **599**, 471–476 (2021).
45. C. C. Pan, F. Winkler, Insights and opportunities at the crossroads of cancer and neuroscience. *Nat. Cell Biol.* **24**, 1454–1460 (2022).
46. Q. Zeng *et al.*, Synaptic proximity enables NMDAR signalling to promote brain metastasis. *Nature* **573**, 526–531 (2019).
47. M. Kaduri *et al.*, Targeting neurons in the tumor microenvironment with bupivacaine nanoparticles reduces breast cancer progression and metastases. *Sci. Adv.* **7**, eabj5435 (2021).
48. D. Yuan *et al.*, RNA Sequencing Dataset. Figshare. <https://doi.org/10.6084/m9.figshare.24447394>. Deposited 1 November 2023.